ISSN 1023-1935, Russian Journal of Electrochemistry, 2021, Vol. 57, No. 7, pp. 681–687. © Pleiades Publishing, Ltd., 2021.
Russian Text © The Author(s), 2021, published in Elektrokhimiya, 2021, Vol. 57, No. 7, pp. 382–389.

Electrical and Dielectric Properties of Sb_2O_3–$PbCl_2$–AgCl Glass System[1]

O. Bošák[a], *, M. Kubliha[a], P. Kostka[b, c], S. Minarik[a], M. Domankova[a], and D. Le Coq[d]

[a] *Faculty of Materials Science and Technology, Slovak University of Technology, Trnava, 91724 Slovakia*

[b] *Laboratory of Inorganic Materials, Institute of Rock Structure and Mechanics of the Czech Academy of Sciences, V Holešovičkách, Prague, 18209 Czech Republic*

[c] *Laboratory of Inorganic Materials, University of Chemistry and Technology Prague Technická, Prague 6, 16628 Czech Republic*

[d] *Université de Rennes, CNRS – ISCR UMR 6226, Rennes, F-35000 France*

**e-mail: ondrej.bosak@stuba.sk*

Received September 30, 2020; revised December 9, 2020; accepted February 14, 2021

Abstract—Electrical and dielectric properties of ternary glasses in the Sb_2O_3–$PbCl_2$–AgCl system were investigated across a broad temperature and frequency range. The studied glass system is interesting since it possesses a high ionic conductivity. The $(Sb_2O_3)_x$–$(PbCl_2)_{100-y-x}$–$(AgCl)_y$ glasses were prepared by melt-quenching method from high purity components. Different batches of these glasses were investigated with varying molar content of both Sb_2O_3 ($45 \le x \le 70$ mol %) and AgCl ($5 \le y \le 25$ mol %). The colour of the prepared chloro-antimonite glasses varies between yellow and brown. The glass transition temperature (T_g) decreases with increasing AgCl concentrations. DC and AC electrical conductivities and complex electrical modulus were measured across a temperature range from room temperature up to 200°C and across a frequency range between 0.2 and 10^5 Hz. The dependence of DC conductivity on temperature follows the so-called Arrhenius-like equation. The DC conductivity at constant temperature significantly increases with increasing AgCl or $PbCl_2$ content. It was found that the activation energy of conduction process decreases with the substitution of $PbCl_2$ by AgCl from 1 eV down to 0.56 eV for $(Sb_2O_3)_{50}$-$(PbCl_2)_{45}$–$(AgCl)_5$ and $(Sb_2O_3)_{50}$–$(PbCl_2)_{25}$–$(AgCl)_{25}$, respectively. The influence of the composition on the AC conductivity of the investigated glasses is also discussed.

Keywords: antimony oxide-based glasses, electrical conductivity, ionic conductivity, complex electrical modulus

DOI: 10.1134/S1023193521070041

INTRODUCTION

Antimony oxide-based glasses, as a major family of heavy metal oxide glasses, show promising potential for applications in nonlinear optical devices such as ultrafast optical switches and/or power limiters [1–4]. They also have potential for application in broadband optical amplifiers operating around at 1.5 μm, and silicate glasses containing antimony were tested for optical amplification in communications in the C-band (1530–1560 nm) [5].

Stable binary glasses are formed in the $(Sb_2O_3)_{1-x}$–$(PbCl_2)_x$ system [6, 7], which enables additions of other oxide compounds such as MoO_3 or TeO_2 and/ormetal halides (CuI, LiCl, $ZnCl_2$), as related in other works [7–15].

The Sb_2O_3–$PbCl_2$–AgCl glass system is particularly interesting due to its high ionic conductivity due to the presence of Ag. In addition to electrical conductivity, these glasses are transparent across a wide optical range (400 nm–6.5 μm) and they thus have a potential for applications in optoelectronics [16].

In this paper, the compositions of the investigated glasses belong to a wide range of compositions for which $[Sb_2O_3] \in (45; 70)$, $[PbCl_2] \in (5; 40)$ and $[AgCl] \in (5; 25)$. The glass transition temperatures of the prepared glasses are given. Moreover, the electrical and dielectric properties of the Sb_2O_3–$PbCl_2$–AgCl glasses across a broad range of temperatures and frequencies are presented. This allows the temperature dependence of DC and AC conductivity as well as the dielectric properties of the glass samples to be investigated.

EXPERIMENTAL

The glasses were prepared using the standard processing steps of melting homogenised mixtures of the starting compounds, fining, cooling, melt casting, and annealing of glass bulks. Starting materials—

[1] Based on the materials of the report at the 15th International Meeting "Fundamental Problems of Solid State Ionics," Chernogolovka, 30.11.–07.12.2020.

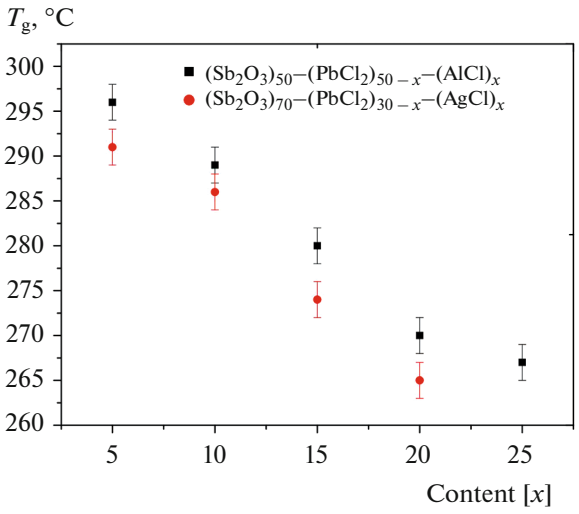

Fig. 1. Glass transition temperature T_g dependence for two glass series: $(Sb_2O_3)_{50}$–$(PbCl_2)_{50-x}$–$(AgCl)_x$ and $(Sb_2O_3)_{70}$–$(PbCl_2)_{30-x}$–$(AgCl)_x$ as a function of AgCl concentration.

99.9% Sb_2O_3 (Acros organics), 99% $PbCl_2$ (Hichem), and 99.9% AgCl (Alfa Aesar)—were thoroughly mixed in an agate mortar and placed into a silica tube. Silica is not an ideal material for preparing this glass as it gradually dilutes in the glass melt. However, it is a better choice than platinum or gold, which both can be attacked by metallic particles resulting from oxidation-reduction reactions during heating of the batch and the glass melting process [16]. The contamination of the melt by SiO_2 can be kept under the limit of detection by EDS semi quantitative chemical analysis if the melting time is kept as short as possible just to obtain a homogeneous glass melt [7]. During the melting process, the tube fills up with vapours from the glass melt which prevent the contact of the melt with ambient air and/or with combustion products from the flame used for heating.

After fining at about 850°C the melt was rapidly cooled down to approximately 600°C and poured on a brass plate preheated to 250°C (near the glass transition temperature T_g). After solidification, the sample was placed into an oven heated at T_g to remove thermally induced stresses. After a few hours at T_g, the temperature of the oven is slowly decreased down to room temperature [17].

The glass transition temperature T_g was measured by heating at a linear slope of 10°C/min using the TA Instruments DSC Q20 differential scanning calorimeter.

Samples for measurements of electrical and dielectric properties were cut and polished, and contact surfaces were coated with a conductive graphite layer. The DC conductivity was determined by measuring the electric current passing through the sample at a constant voltage of 10 V by Novocontrol Concept 90, across a temperature of 20–200°C. The current was measured by the Keithley 6517B picoammeter and the temperature was controlled by a Pt/PtRh thermocouple with an accuracy of ±1°C. Temperature dependence of the DC conductivity was measured during the phase when the temperature increased at a rate of 5°C/min [16].

The AC measurements (from 20 up to 150°C) were performed using the LCR Hi-tester Hioki 3522-50 at a frequency range 100 Hz–100 kHz. The measurements were performed in steps of 10°C after the temperature remained constant for 20 min [9, 18, 19]. Typically, as the frequency increases, the influence of electron transport processes increases, so at higher frequencies it is possible to see the influence of chemical elements for which different valence states are possible (Sb^{3+}, Sb^{5+}, W^{6+}, W^{5+}).

RESULTS

The acronyms of the respective glass compositions and their corresponding compositions expressed in molar percentages are shown in Table 1. The table summarizes also the electric and dielectric properties described in following text. The dependencies of the transition temperature T_g on the AgCl content in the studied Sb_2O_3–$PbCl_2$–AgCl glasses are shown in Fig. 1. The T_g values decrease with increasing AgCl content in glasses with both 50 and 70 mol % Sb_2O_3. The temperature dependence of DC conductivity, σ_{dc}, of the investigated glasses is presented in Fig. 2. At temperature sranging between room temperature and 200°C the observed dependences follow Arrhenius-like equation

$$\sigma_{dc} = \sigma_0 \exp\left(E_{dc}/kT\right), \quad (1)$$

where σ_0 is the pre-exponential factor, E_{dc} is the conduction activation energy, k is the Boltzmann constant, and T is the thermodynamic temperature. The determined parameters of Eq. (1) for the linear parts of the recorded temperature dependences of DC conductivity are summarized in Table 1.

The AC conductivity σ_{ac} of Sb_2O_3–$PbCl_2$–AgCl glasses increases with increasing temperature and frequency. In Fig. 3, frequency dependencies of AC conductivity measured at 150°C are presented. AC conductivity frequency dependency can be described using the following formula

$$\sigma_{ac} = \sigma_{01} + Af^n, \quad (2)$$

where f is the frequency, and A and n are the parameters. The value of σ_{01} corresponds to DC conductivity, and its values for the temperature of 150°C are shown in Table 1. The value of σ_{01} is subject to an error due to the fact that it is an extrapolated value and also that the contribution of other carriers of electric charge (for example electrons) is more pronounced at higher frequencies in AC measurements than in DC measure-

Table 1. Parameters of Sb_2O_3–$PbCl_2$–AgCl glasses: glass composition acronym, composition in mol %, conduction activation energies (E_{dc}), pre-exponential factors (σ_0), and electrical conductivity (σ_{dc}) at 150°C, AC conductivity frequency dependency parameters calculated by using the approximation of equation $\sigma_{ac}(f) = \sigma_{01} + A f^n$ from measurement values at 150°C

Sample	Symbol	Sb_2O_3, %	$PbCl_2$, %	AgCl, %	E_{dc}, eV	$\sigma_{dc} \times 10^9$ (150°C), S/m	$\sigma_{01} \times 10^9$ (150°C), S/m	$A \times 10^9$ (150°C), S/m	n (150°C)	E_τ, eV
A45-05	■	50	45	05	1.00 ± 0.01	2.12	9.6 ± 1.7	0.11 ± 0.01	0.77 ± 0.02	
A40-10	●	50	40	10	0.91 ± 0.01	37.20	54 ± 4	1.3 ± 0.1	0.68 ± 0.01	
A35-15	▲	50	35	15	0.76 ± 0.01	598.8	592 ± 11	8.9 ± 0.5	0.65 ± 0.01	0.76 ± 0.03
A30-20	▼	50	30	20	0.66 ± 0.01	6583	8480 ± 60	45 ± 1	0.61 ± 0.01	0.63 ± 0.04
A25-25	◆	50	25	25	0.56 ± 0.03	36560	63700 ± 800	254 ± 40	0.56 ± 0.02	0.57 ± 0.09
B 25-05	■	70	25	05	0.98 ± 0.03	11.03	27 ± 3	0.50 ± 0.06	0.69 ± 0.01	
B20-10	●	70	20	10	0.90 ± 0.01	38.45	65 ± 5	1.3 ± 0.1	0.69 ± 0.01	
B15-15	▲	70	15	15	0.78 ± 0.01	334.2	333 ± 8	5.9 ± 0.3	0.66 ± 0.01	0.82 ± 0.21
B10-20	▼	70	10	20	0.70 ± 0.01	1057	1360 ± 30	10 ± 1	0.68 ± 0.01	0.71 ± 0.05
B05-25	◆	70	05	25	0.74 ± 0.01	383.8	598 ± 20	6.4 ± 0.4	0.70 ± 0.01	0.74 ± 0.02
D20-20	▲	60	20	20	0.59 ± 0.02	15851	42700 ± 300	70.6 ± 4	0.67 ± 0.01	0.49 ± 0.05
D20-25	▼	55	20	25	0.67 ± 0.02	12772	21900 ± 300	102 ± 7	0.64 ± 0.01	
D20-30	◆	50	20	30	0.61 ± 0.02	10943	30200 ± 200	84 ± 8	0.62 ± 0.01	0.63 ± 0.03
E30-05	■	65	30	05	0.93 ± 0.01	63.44	84 ± 4	2.0 ± 0.1	0.63 ± 0.01	
E30-10	●	60	30	10	0.85 ± 0.01	623.7	670 ± 10	9.3 ± 0.3	0.61 ± 0.01	
E30-15	▲	55	30	15	0.74 ± 0.01	6866	10460 ± 80	53 ± 3	0.60 ± 0.01	0.70 ± 0.03
E30-20	▼	50	30	20	0.73 ± 0.01	20840	27200 ± 300	108 ± 8	0.64 ± 0.01	
E30-25	◆	45	30	25	0.57 ± 0.01	23635	107844 ± 1500	647 ± 70	0.54 ± 0.02	

ments (mainly ionic conductivity in the investigated glasses). Therefore in some cases the σ_{dc} and σ_{01}values may differ significantly from each other. The parameter A increases and the exponent n slightly decreases with increasing $PbCl_2$ and AgCl contents.

The dielectric response was studied using modular spectroscopy. Complex electrical modulus M^* was introduced [20–22] as the reciprocal value of the complex permittivity ε^* by the equation

$$M^* = M' + jM'' = \left(\varepsilon_r^*\right)^{-1}. \quad (3)$$

The measured modular spectra, i.e. the dependencies of complex electrical modulus in complex plane, are shown in Fig. 4. At lower AgCl content, the shapes of modular spectra can be characterized as semicircles with a centre just below the real axis with linear tails appearing at high frequencies. In these cases, dielectric relaxation can be characterized by a relatively narrow range of relaxation times. At higher AgCl content, the centres of the semicircles shift more under real axis. Consequently, the range of relaxation times expands.

The relaxation times as a function of temperature $\tau = \tau(T)$ were calculated as reciprocal value of angular frequency $1/(2\pi f_m)$, where f_m is the frequency of maxima M'' obtained from frequency dependency of the imaginary part of complex electric modulus. As an example, Fig. 5 shows these dependencies of M'' for glass E30-15 at various temperatures. For glasses where relaxation time values could be determined, the temperature dependencies of relaxation times follows the Arrhenius equation (see Fig. 6).

Activation energy E_τ for Arrhenius-type dielectric relaxation was determined using the expression

$$\tau = \tau_0 \exp\left(-E_\tau / kT\right), \quad (4)$$

where τ_0 is the pre-exponential factor, E_τ is the conduction activation energy, k is the Boltzmann constant, and T is the thermodynamic temperature. The value of E_τ correlates with the value of E_{dc} (Table 1), i.e. the activation energy of the dielectric relaxation is

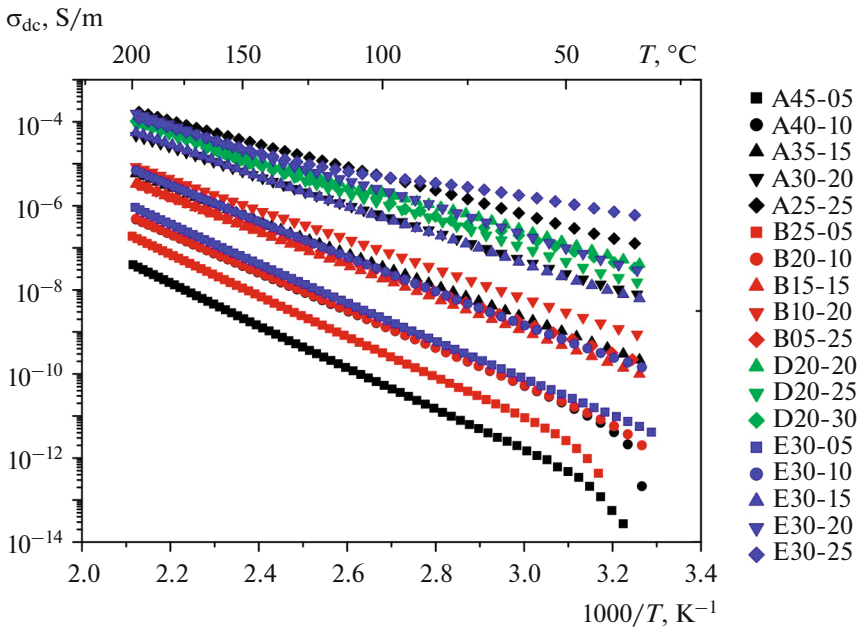

Fig. 2. DC conductivity temperature dependency curves of Sb_2O_3–$PbCl_2$–AgCl glasses measured at a temperature range of 25–200°C. Glass samples corresponding to the individual plotted data are indicated in the figure.

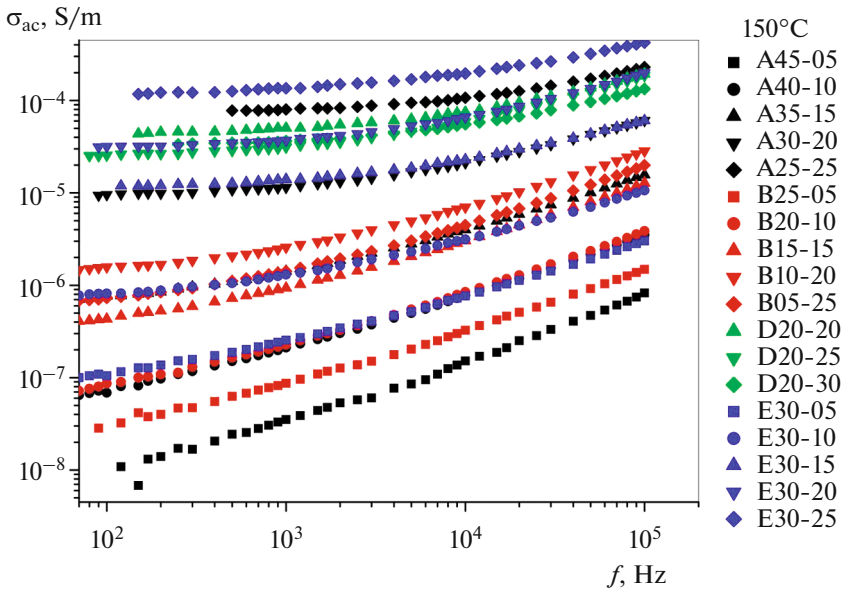

Fig. 3. AC conductivity frequency dependency curves of Sb_2O_3–$PbCl_2$–AgCl glasses measured at 150°C. Glass samples corresponding to the individual plotted data are indicated in the figure.

affected by transport of the same type of electric charge.

DISCUSSION

The decrease of T_g values with increasing AgCl content in investigated glasses corresponds to the AgCl roleplays as a modifier in the antimonite glass network. According to [16], the increase in the molar concentration of AgCl leads to decrease of T_g values due to the formation of weaker Ag–Cl chemical bonds instead of stronger Sb–O bonds. The glass can accept only certain amount of modifiers without deterioration of the glassy network stability. As a consequence, the glass stability and density decrease significantly at high AgCl concentrations. As far as DC conductivity is

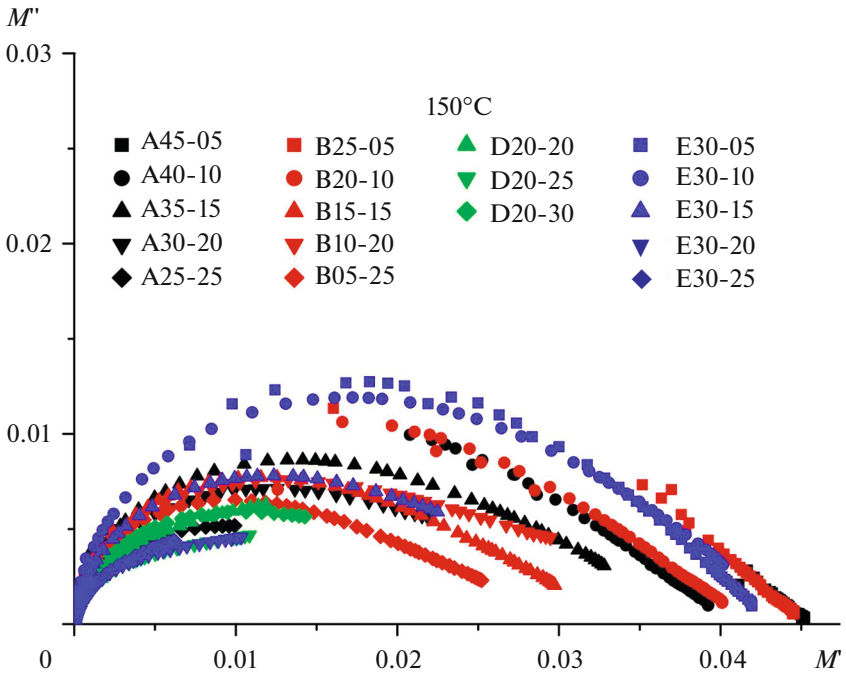

Fig. 4. Modular diagrams of Sb_2O_3–$PbCl_2$–AgCl glasses at 150°C. Glass samples corresponding to the individual plotted data are indicated in the figure.

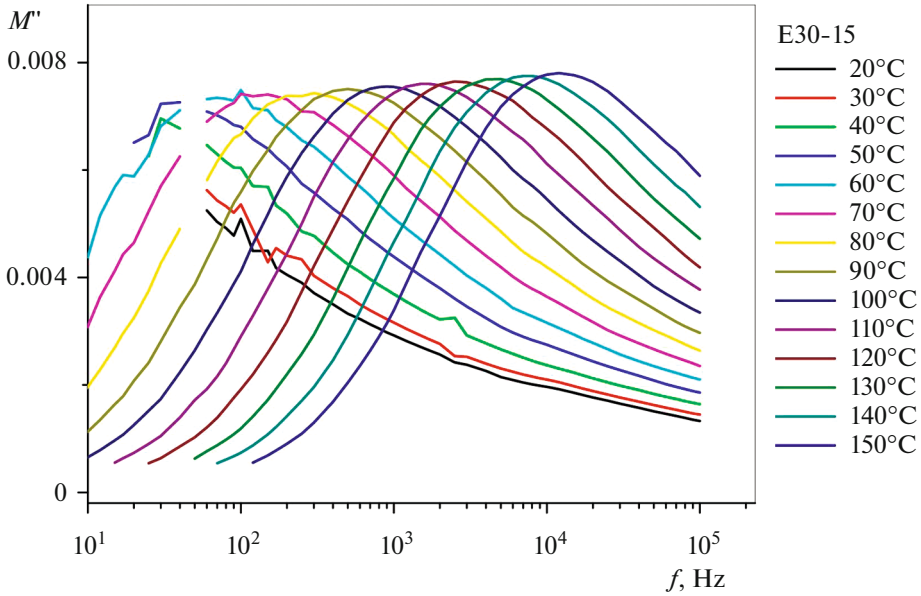

Fig. 5. Frequency dependency of the imaginary part of complex electric modulus M'' for $(Sb_2O_3)_{55}$–$(PbCl_2)_{30}$–$(AgCl)_{15}$ glass (E30-15) at various temperatures. Colours in the figure correspond to different temperatures.

concerned, temperature dependencies can be well described by the Arrhenius law with a single dominant mechanism of electric charge transport. In terms of the glass composition, polaronic conductivity Sb^{3+}–Sb^{5+} and/or ionic conductivity by means of Ag^+, or Cl^- ions, respectively, could be considered as probable transport mechanisms. Transition from polaronic conductivity to ion conductivity mediated by Ag^+ ions at lower concentrations of AgO (>0.1 mol %) has been reported recently [23]. It could be assumed that Ag^+ ions are dominant charge carriers in Sb_2O_3–$PbCl_2$–AgCl glasses. The DC conductivity values increase

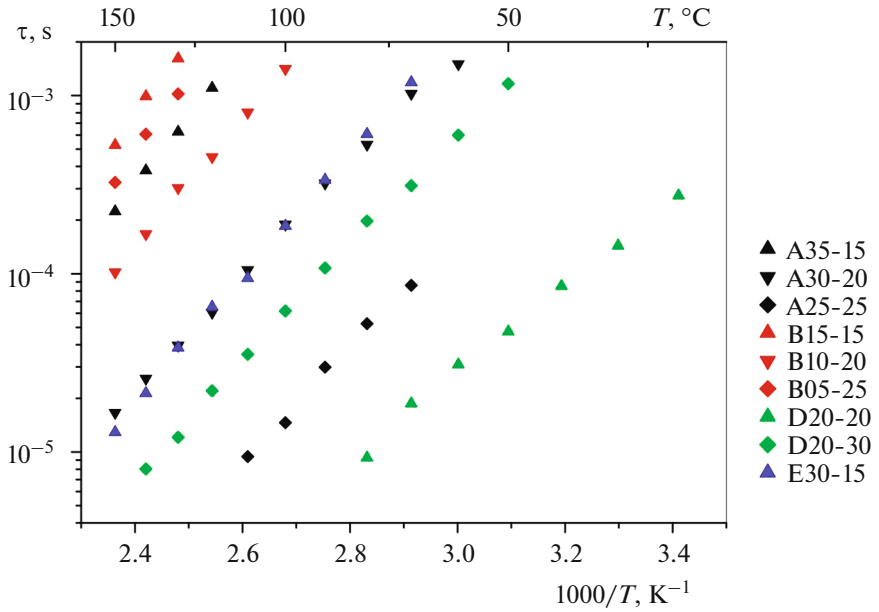

Fig. 6. Relaxation times of selected Sb_2O_3–$PbCl_2$–AgCl glasses in dependence on temperature. Glass samples corresponding to the individual plotted data are indicated in the figure.

and the DC conductivity activation energy decreases with increasing AgCl content. The contribution of Cl^- ions to DC conductivity is probably not significant. The DC conductivity values also increase with higher $PbCl_2$ content. It is important, that this compound causes the increase of mobility of ions due to a relaxation of the glass network and an increase of the molar volume [16]. The authors investigated the possibility of electric transport using Cl^- ions in detail in a similar glass system of Sb_2O_3–$PbCl_2$–LiCl [14]. Their analysis showed that the influence of Cl^- ions on electrical conductivity is negligible. It means that the DC conductivity increases at higher AgCl and $PbCl_2$ contents due to the expansion of the glass network lead to an increase of the ion mobility. Moreover, in the case of AgCl an increase of the concentration of charge carriers occurs. The glass network relaxation is connected with a decrease of activation energies of DC conductivity in an interval ranging from 1 eV (A45-05) to 0.56 eV (A25-25). The A25-25 glass also reaches the highest value of conductivity at 150°C.

At measured temperatures, AC conductivity increases with increasing angular frequency and changes according to the power-law described by relation (2). The changing values of σ_{01} and A shown in Table 1 suggest that the dominant underlying mechanism of AC conductivity is the transport of the same type of electric charge as in the case of DC conductivity (σ_{dc} (150°C) in Table 1). The shape of the measured modular spectra (Fig. 4) indicates significant influence of ion movement. Also the activation energy of dielectric relaxation corresponds to the activation energy of DC conductivity. This also means that the influence of Ag^+ ions transport is significant.

CONCLUSIONS

The results obtained by electrical measurements and the observed dependencies of the parameters of the studied materials show that the conductivity of Sb_2O_3–$PbCl_2$–AgCl glasses show an Arrhenius-type behaviour. The dominant mechanism of charge transport in the investigated glasses is an ionic mechanism involving Ag^+ ions. On the other hand, the contribution of Cl^- ions and/or electrons to the transport of electric charge in these materials is less significant.

The values of direct electric conductivity are spread across a range spanning 5 orders of magnitude. The highest value of DC conductivity, around 3.6×10^{-5} S m^{-1} at 150°C with a corresponding activation energy of 0.56 ± 0.03 eV, was obtained for the $(Sb_2O_3)_{50}$–$(PbCl_2)_{25}$–$(AgCl)_{25}$ glass. Positive influence of the addition $PbCl_2$ on electric mobility of the charge carrier Ag^+ has been highlighted. The transport of electric charge by Ag^+ ions has also an effect on values of alternate electric conductivity and dielectric relaxation of glasses.

FUNDING

This work was supported by the Slovak Science Foundations, projects VEGA 1/0235/18, VEGA 1/0144/20, APVV SK-FR-19-0007, and APVV DS-FR-19-0036, P. Kostka acknowledges the Czech Science Foundation—project no. 19-07456S and the Ministry of Education, Youth and

Sports of the Czech Republic—project no. 8X20053.This publication is partially supported by the European Union through the European Regional Development Fund (ERDF), the Ministry of Higher Education and Research, the French region of Brittany and Rennes Métropole.

CONFLICT OF INTERESTS

The authors declare that they have no conflict of interest.

INFORMATION OF PERSONAL CONTRIBUTIONS OF AUTHORS

D. Le Coq prepared samples of glasses for experiments and performed DSC experiments. O. Bošák and M. Kubliha performed measurements of direct electrical conductivity and modular spectra. S. Minarik analysed modular spectra. O. Bošák, M. Kubliha, M. Domankova, and P. Kostka wrote the first draft of the manuscript. All authors edited the manuscript and approved the final version.

ADDITIONAL INFORMATION

Authors ORCID ID. O. Bošák (0000-0001-6467-5398), M. Kubliha (0000-0003-4987-6233), P. Kostka (0000-0003-2868-1322), S. Minarik (0000-0002-6851-0053), M. Domankova(0000-0002-0595-1943), D. Le Coq (0000-0001-7898-3463).

REFERENCES

1. Dubois, B., Aomi, H., Videau, J.J., Portier, J., and Hagenmuller, P., New oxyhalide glasses involving Sb_2O_3, *Mat. Res. Bull.,* 1984, vol. 19, no. 10, p. 1317.
2. Zavadil, J., Ivanova, Z.G., Kostka, P., Hamzaoui, M., and Soltani, M.T., Photoluminescence study of Er-doped zinc-sodium-antimonite glasses, *J. Alloy. Compd.,* 2014, vol. 611, p. 111.
3. Soltani, M.T., Hamzaoui, M., Houhou, S., Touiri, H., Bediar, L., Ghemri, A.M., and Petkova, P., Physical characterization of Sb_2O_3–M_2O–MoO_3 (M = Li, K) new glasses, *Acta Phys. Pol. A,* 2013, vol. 123, p. 227.
4. Hamzaoui, M., Azri, S., Soltani, M.T., Lebullenger, R., and Poulain, M., Thermal and elastic characterization of Sb_2O_3–Na_2O–ZnO glasses, *Phys. Scr.,* 2013, vol. 157, p. 014029. https://doi.org/10.1088/0031-8949/2013/T157/014029
5. Minelly, J. and Ellison, A., Applications of antimony-silicate glasses for fiber optic amplifiers, *Opt. Fiber Technol.,* 2002, vol. 8, p. 123.
6. Dubois, B., Videau, J.J., Couzi, M., and Portier, J., Structural approach of the (x$PbCl_2$-(1-x)Sb_2O_3) glass system, *J. Non-Cryst. Solids,* 1986, vol. 88, p. 355.
7. Bošák, O., Kostka, P., Minárik, S., Trnovcová, V., Podolinčiaková, J., and Zavadil, J., Influence of composition and preparation conditions on some physical properties of TeO_2–Sb_2O_3–$PbCl_2$ glasses, *J. Non-Cryst. Solids,* 2013, vol. 377, p. 74.
8. Goumeidane, F., Legouera, M., Iezid, M., Poulain, M., Nazabal, V., and Lebullenger, R., Synthesis and physical properties of glasses in the Sb_2O_3–$PbCl_2$–MoO_3 system, *J. Non-Cryst. Solids,* 2011, vol. 357, p. 3572.
9. Labaš, V., Poulain, M., Kubliha, M., Trnovcová, V., and Goumeidane, F., Electrical, dielectric and optical properties of Sb_2O_3–$PbCl_2$–MoO_3 glasses, *J. Non-Cryst. Solids,* 2013, vol. 377, p. 66.
10. Macháček, J., Kostka, P., Liška, M., Zavadil, J., and Gedeon, O., Calculation and analysis of vibrational spectra of $PbCl_2$–Sb_2O_3–TeO_2 glass from first principles, *J. Non-Cryst. Solids,* 2011, vol. 357, p. 2562.
11. Gedikoglu, N., Ersundu, M.C., Kostka, P., Basinova, N., and Ersundu, A.E., Investigating the influence of transition metal oxides on temperature dependent optical properties of $PbCl_2$–TeO_2 glasses for their evaluation as transparent large band gap semiconductors, *J. Alloys Compd.,* 2018, vol. 748, p. 687.
12. Poirier, G., Poulain, M., and Poulain, M., Copper and lead halogeno-antimoniate glasses, *J. Non-Cryst. Solids,* 2001, vol. 284, p. 117.
13. Cozic, S., Bréhault, A., Usuki, T., and Le Coq, D., GeS_2–Ga_2S_3–LiCl glass system: electrical conductivity and structural considerations, *Int. J. Appl. Glass Sci.,* 2016, vol. 7, no. 4, p. 513.
14. Castro, A., Bréhault, A., Carcreff, J., Bošák, O., Kubliha, M., Trnovcová, V., Dománková, M., Šiljegović, M., Calvez, L., Labaš, V., and Le Coq, D., Lithium and lead chloride antimonate glasses, *J. Non-Cryst. Solids,* 2018, vol. 499, p. 66.
15. Sahar, M.R., Ahmed, M.M., and Holland, D., The crystallisation of Sb_2O_3–$PbCl_2$–$ZnCl_2$ glasses, *Phys. Chem. Glasses,* 1990, vol. 31, no. 3, p. 126.
16. Yezli, D., Legouera, M., El Abdi, R., Poulain, M., and Burgaud, V., Mechanical, thermal, and optical properties of new chloroantimonite glasses in the Sb_2O_3–$PbCl_2$–AgCl system, *Mat. Sci.,* 2016, vol. 52, no. 1, p. 33.
17. Kubliha, M., *Investigating Structural Changes and Defects of Non-Metallic Materials via Electrical Methods*, 1 st ed., Dresden: Forschungszentrum Dresden-Rossendorf, 2009.
18. Kalužný, J., Kubliha, M., Labaš, V., Poulain, M., and Taibi, Y., Electrical and dielectrical properties of Sb_2O_3–V_2O_5–K_2O glasses, *J. Non-Cryst. Solids,* 2009, vol. 355, nos. 37–42, p. 2031.
19. Kubliha, M., Soltani, M.T., Trnovcová, V., Legouera, M., Labaš, V., Kostka, P., Le Coq, D., and Hamzaoui, M., Electrical, dielectric, and optical properties of Sb_2O_3–Li_2O–MoO_3 glasses, *J. Non-Cryst. Solids,* 2015, vol. 428, p. 42.
20. Moynihan, C.T., Boesch, L.P., and Laberge, N.L. Decay function for electric-field relaxation in-vitreous ionic conductors, *Phys. Chem. Glasses,* 1973, vol. 14, p. 122.
21. Molak, A., Paluch, M., Pawlus, S., Klimontko, J., Ujma, Z., and Gruszka, I., Electric modulus approach to the analysis of electric relaxation in highly conducting $(Na_{0.75}Bi_{0.25})(Mn_{0.25}Nb_{0.75})O_3$ ceramics, *J. Phys. D: Appl. Phys.,* 2005, vol. 38, p. 1450.
22. Davidson, D.W. and Cole, R.H., Dielectric relaxation in glycerine, *J. Chem. Phys.,* 1950, vol. 18, p. 1417.
23. Ashok, J., Kostrzewa, M., Ingram, A., Venkatramaiah, N., Srinivasa Reddy, M., Ravi Kumar, V., Piasecki, M., and Veeraiah, N., Structural and dielectric features of silver doped sodium antimonate glass ceramics, *J. Alloy. Compd.,* 2019, vol. 791, p. 278.